Fabrication and Properties of TiO_2 Photo-Catalytic Coatings by Thermal Spraying with TiO_2-Al Agglomerated Powder

Akira OHMORI*, Souta MATSUSAKA and Yoshimasa TOKI*****

Abstract

In the present study, anatase TiO_2 photo-catalytic coatings were fabricated by plasma and HVOF spraying. In order to prevent the transformation from anatase to rutile phase, lower heat input conditions were adopted. For the improvement of bondability between coatings and substrate, anatase TiO_2-Al agglomerated powder was used for the experiment. The microstructures of the coatings were characterized with SEM and XRD analysis, and the photo-catalytic characteristics of coatings were evaluated by the decomposition rate of acetaldehyde gas. Due to the addition of aluminum, thick coatings were formed even at lower heat input conditions in both plasma and HVOF spraying. The results of XRD analysis for the plasma sprayed coatings, however, indicated the disappearance of anatase phase and deoxidization of TiO_2 to Ti_3O_5 or magneli phase. On the other hand, high anatase/rutile ratio and high photo-catalytic efficiency were achieved for the coatings formed by HVOF spraying. The temperature measurements of flying particles were also carried out using DPV-2000. As a result, significant increases in temperature of TiO_2-Al particles were observed compared with the case of using pure TiO_2 particle. These results suggest that a chemical reaction between TiO_2 and Al occurs during thermal spraying.

KEY WORDS : (Photo-catalyst), (TiO_2-Al agglomerated powder), (Plasma spraying), (HVOF), (Acetaldehyde)

1. Introduction

It is well-known that the semiconductor, titanium dioxide (TiO_2), has photo-chemical characteristics[1]. In recent years, applications of TiO_2 photo-catalyst to environmental purification, such as decomposition of organic compound in polluted air and wastewaters, have been increasing[2, 3].

TiO_2 shows three different crystal structures, that is, anatase, rutile and brookite type. In terms of photo-catalytic efficiency, anatase is superior to the others[4]. However, anatase is meta-stable and will be transformed to rutile after an annealing treatment about at 1100K. Therefore, TiO_2 photo-catalyst coatings are generally prepared by low temperature processes such as dipping, spraying and sol-gel method[5-7].

Thermal spraying is also one of the most promising techniques to produce TiO_2 photo-catalytic coatings. The thermal spraying process is non-equilibrium involving rapid cooling, so that meta-stable phases are often formed in the coatings. It follows that the thermal spraying is applicable to fabrication of anatase TiO_2 coatings. In the previous paper[8], we reported that the control of heat input is essential to prevent the transformation of TiO_2 from anatase to rutile phase. On the other hand, low heat input conditions during thermal spraying generally causes poor coatings.

To produce sufficiently thick TiO_2 coatings with high photo-catalytic efficiency, anatase TiO_2-Al agglomerated powders are used for thermal spraying in the present study. The effects of addition of aluminum on the fabrication and characteristics of TiO_2 coatings are investigated. The chemical reactions between TiO_2 and Al during thermal spraying are also discussed.

2. Materials and experimental procedures

2.1 Materials

† Received on December 18, 2000
* Professor
** Post doctoral research fellow
*** Graduate student

Transactions of JWRI is published by Joining and Welding Research Institute of Osaka University, Ibaraki, Osaka 567-0047, Japan.

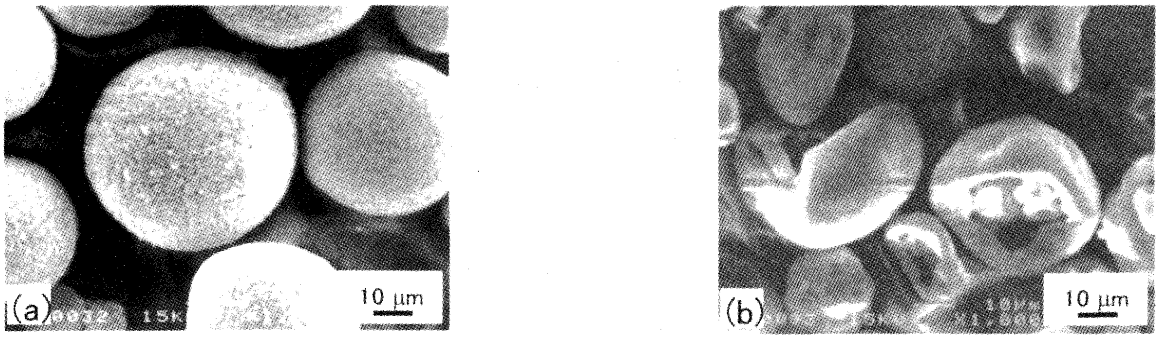

Fig. 1 SEM images of two kinds of agglomerated powders. (a) TiO_2 powder, (b) TiO_2-20mass%Al powder.

Two kinds of agglomerated powders, anatase TiO_2 and anatase TiO_2-20mass%Al, were used for the experiment. The mean particle sizes were 33.7 μm (TiO_2) and 30.3 μm (TiO_2-Al), and the original grain sizes of TiO_2 and Al were 0.2 μm and 6.1 μm, respectively. The morphologies of these powders are shown in Fig. 1. Stainless steel (SUS304, 50 x 60 x 3 (mm)) was used as substrate.

2.2 Thermal spraying

Plasma spraying (PlasmaDyne) and HVOF spraying (JetKote) were used to deposit TiO_2 coatings. In both cases, spraying was performed in the ambient air. Table 1 and Table 2 summarize the experimental conditions for plasma and HVOF spraying, respectively. Arc current and fuel gas pressure were changed to investigate the effect of heat input on the structure and photo-catalytic efficiency of the coatings. During the spraying, the mean temperatures of flying particles were also measured by DPV-2000 (TECNAR).

Table 1 Plasma spray conditions.

Ar pressure (MPa)	0.42
He pressure (MPa)	0.21
Spraying distance (mm)	100
Spraying atmosphere	Air
Arc current (A)	250~500
Arc voltage (V)	28~30
Traverse speed of gun (mm/s)	90

Table 2 HVOF spray conditions.

O_2 pressure (MPa)	0.55
Fuel gas pressure (MPa)	0.20~0.40
Carrier gas pressure (MPa)	0.15
Spraying distance (mm)	100
Traverse speed of gun (mm/s)	90

2.3 Characterization of the coating

The structure of the coating was characterized by X-ray diffraction (XRD) analysis. Anatase ratio expressed as the relative content of anatase TiO_2 in the coating, R_a, was estimated from the following equation,

$$R_a = I_{A(101)} / (I_{A(101)} + I_{R(101)}) \quad (1)$$

where $I_{A(101)}$ and $I_{R(101)}$ are diffraction intensities of the anatase (101) peak and rutile (101) peak, respectively. The microstructure of the TiO_2 coating was examined by scanning electron microscopy (SEM).

2.4 Evaluation of photo-catalytic property of the coating

In order to characterize the photo-catalytic property of the coating, decomposition tests of acetaldehyde gas were carried out. The experimental set-up is illustrated in Fig. 2. The volume of the container was 2 l. After the container was filled with acetaldehyde gas at 100 ppm, the ultraviolet lamp with 360 nm wave length was switched on. The intensity of the light at the sample surface was 1 mW/cm^2. The concentration of acetaldehyde gas was measured with a gas detector after a certain time interval. The decay characteristics of acetaldehyde gas follows the ex-

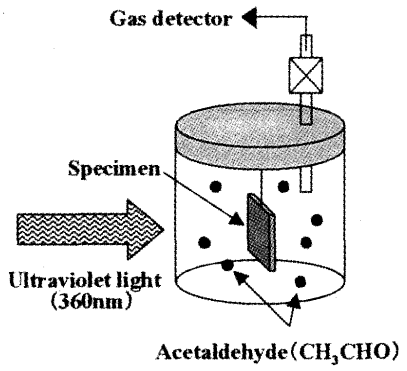

Fig. 2 Schematic illustration of experimental set-up for decomposition test of acetaldehyde gas.

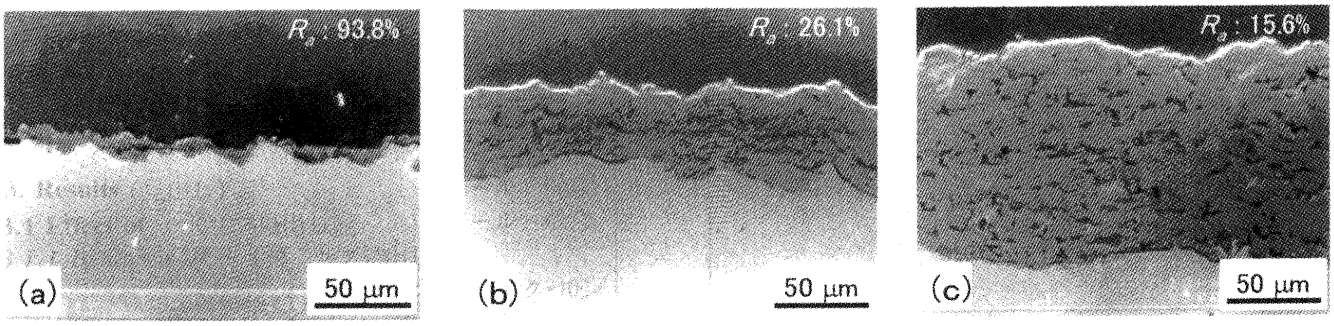

Fig. 3 Cross-sectional microstructures of coatings plasma sprayed with TiO_2 powder at the arc current of (a) 300 A, (b) 350 A, (c) 400 A.

ponential rule[8], as shown in eq. (2),

$$N = N_0 \exp(-t / \tau) \qquad (2)$$

where N and N_0 are the concentration at time t and initial concentration, respectively. τ is a time constant related to the decay speed, and the lower the value of τ, the more rapid is the decomposition of acetaldehyde gas. Therefore, τ was used as a characteristic decay time to evaluate the photo-catalytic efficiency of the coating.

3. Results and discussion

3.1 Structures of the coatings fabricated by plasma spraying

Figure 3 shows the cross-sectional microstructures of coatings sprayed with pure TiO_2 powder under the condition of arc currents of 300, 350 and 400 A, respectively. Anatase ratio, R_a, in each coating is also shown in Fig. 3. In the case of arc current of 300 A, R_a indicates a very high value which is over 90 % because of low heat input. However, the coating thickness decreased as the arc current was reduced, and poor coating was formed at the arc current of 300 A (also see Fig. 4). Therefore, it was considered that in this case most of the flying particles were non-melted and not able to adhere to the substrate.

On the other hand, Fig. 5 shows the mean thickness of the coatings fabricated from TiO_2-Al powder under the same spray conditions as mentioned above. By comparison between Fig. 4 and Fig. 5, it is clearly recognized that the coating thickness increases in every spray condition. In particular, at the arc current of 300 A, a thick coating which was about 50 μm could be deposited. Figure 6 shows the XRD patterns of these coatings. As can be seen in Fig. 6, it was observed that Ti_3O_5 and magneli phases were formed in the coatings. These results suggest that flying TiO_2 particles were deoxidized by aluminum during spraying. However, the formation of Al_2O_3 was not observed.

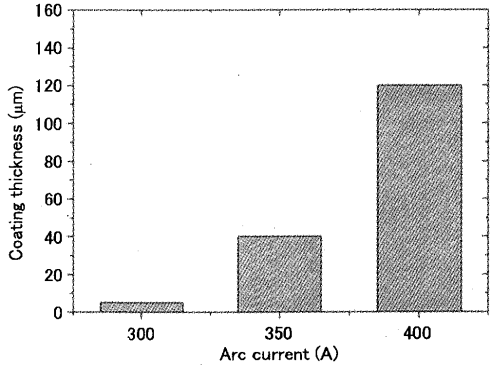

Fig. 4 Effect of arc current on thickness of coating sprayed with TiO_2 powder.

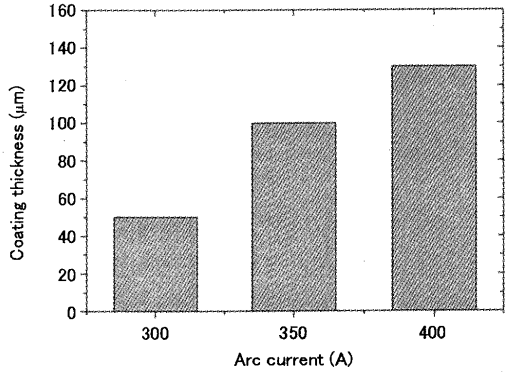

Fig. 5 Effect of arc current on thickness of coating sprayed with TiO_2-Al powder.

Although the reason of disappearance of Al_2O_3 is not clear at present, the formation of amorphous phase may be possible.

The measurements of the mean temperatures of flying particles were carried out for both powders using DPV-2000. The temperature profiles at the arc current of 500 A are shown in Fig. 7. These figures clearly indicate the temperature increase (about 900 K) of particles because of the addition of aluminum. It is considered that the heat generation is due to the chemical reaction between TiO_2 and Al, which is, for example, written as follows,

$$9TiO_2 + 2Al \rightarrow 3Ti_3O_5 + Al_2O_3. \qquad (3)$$

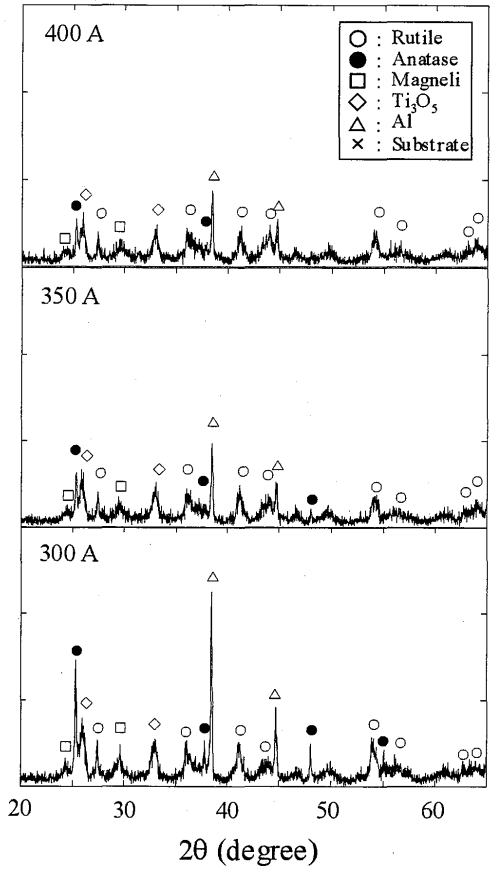

Fig. 6 X-ray diffraction patterns of coatings sprayed with TiO_2- Al powder at various arc currents.

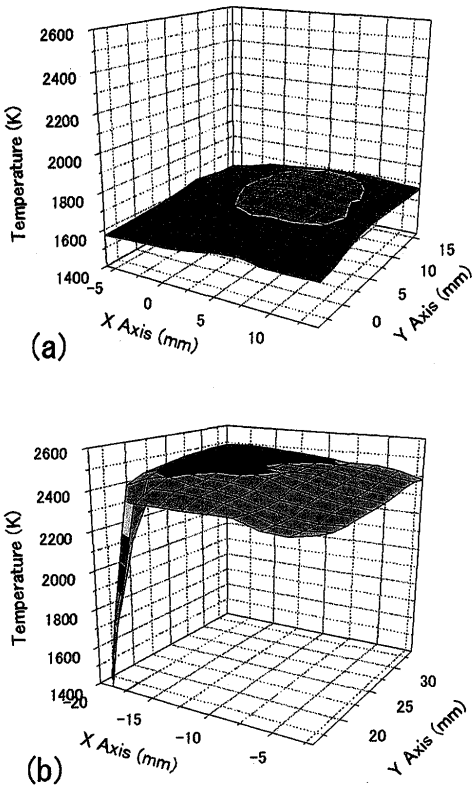

Fig. 7 Temperature profiles of flying particles at the surface of substrate (Arc current : 500 A). (a) TiO_2 powder, (b) TiO_2-Al powder.

This phenomenon, therefore, also suggests deoxidization of TiO_2 to Ti_3O_5 or magneli phase.

3.2 Structures of the coatings fabricated by HVOF spraying

Figure 8 shows the cross-sectional microstructures of coatings sprayed with pure TiO_2 powder under the condition of fuel gas pressure of 0.35 and 0.40 MPa, respectively. In the case of gas pressure of 0.35 MPa, a coating was hardly deposited as shown in Fig. 8 (a). A coating with 20 μm thickness could be deposited at 0.40 MPa. By comparison between Fig. 3 (b), (c) and Fig 8 (b), it is found that a coating sprayed by HVOF has higher anatase ratio than that by plasma spraying. These results are due to the lower heat input and higher particles speed in HVOF spraying process.

Figure 9 shows surface morphologies and cross-sectional microstructures of coatings sprayed with TiO_2-Al powder under the condition of lower fuel gas pressure of 0.20 and 0.25 MPa. As can be seen in Fig. 9 (b) and (d), relatively thick (about 50 μm) coatings with high anatase ratio were

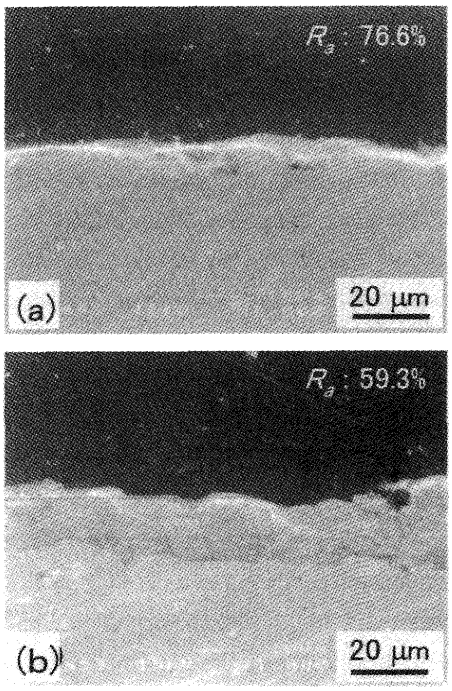

Fig. 8 Cross sectional microstructures of coatings HVOF sprayed with TiO_2 powder at the fuel gas pressure of (a) 0.35 MPa, (b) 0.40 MPa.

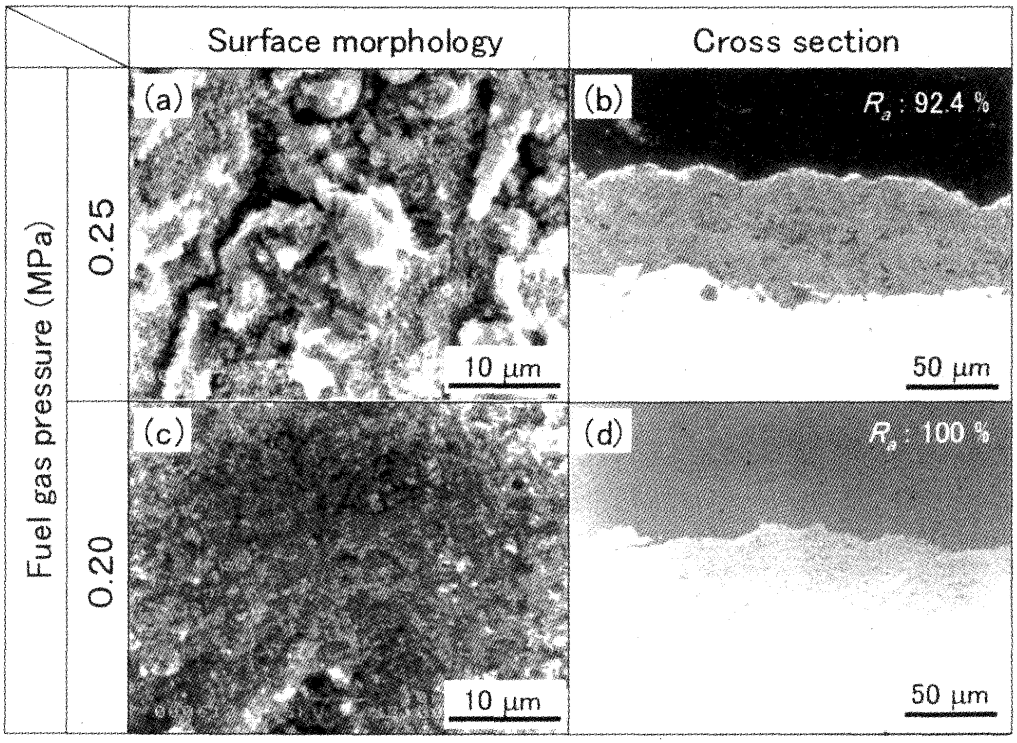

Fig. 9 Surface morphologies and cross-sectional microstructures of the coatings HVOF sprayed with TiO_2-Al powder.

formed. Figure 9 (a) and (c) indicate that the surfaces are covered with powder-like TiO_2 particles with higher R_a values. Such surfaces are probably formed by the following mechanisms, that is, the flying particles with high speed collide with substrates, and then the agglomerated powders are crushed to the original grains and adhere onto the substrates. In this process, melted aluminum plays the role of 'binder'. From the point of view of photo-catalyst, these coatings are most suitable, because they have large effective areas for photo-chemical reaction.

3.3 Decomposition characteristics of acetaldehyde gas

Figure 10 shows typical results of decay characteristics of acetaldehyde concentration. This experiment was performed using pure anatase and rutile TiO_2 powders which were set in petri dish with 30 cm^2 (same area as sprayed specimen). In this case, characteristic decay times, τ, were 0.56 h for anatase and 1.8 h for rutile, respectively.

Table 3 shows τ of coatings fabricated from TiO_2 and TiO_2-Al powders by plasma spraying. It was found that the photo-catalytic performance was improved with reduction of arc current for both powders. However, the decomposition rates of specimens from TiO_2-Al powder were worse by two order than that from anatase TiO_2 powder. It is considered that these results are due to the formation of Ti_3O_5

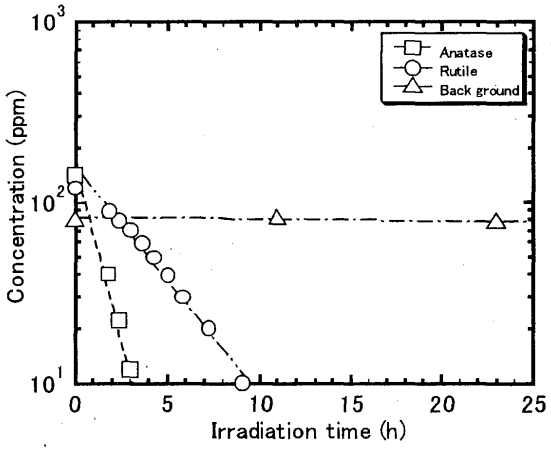

Fig. 10 Decay characteristics of acetaldehyde concentration by pure anatase and rutile TiO_2 powders.

Table 3 Characteristic decay times, τ, of the coatings fabricated from TiO_2 and TiO_2-Al powders at various arc currents.

Arc current (A) / Time constant (h)	TiO_2			TiO_2 -Al		
	300	350	400	300	350	400
τ	0.29	0.61	0.77	77	99	114

Table 4 Characteristic decay times, τ, of the coatings fabricated from TiO_2 and TiO_2-Al powders at various fuel gas pressures.

Fuel gas pressure (MPa) / Time constant (h)	TiO_2		TiO_2 -Al	
	0.35	0.40	0.20	0.25
τ	0.45	0.46	0.60	1.79

and magneli phase in TiO_2-Al system.

Table 4 shows τ of coatings fabricated from TiO_2 and TiO_2-Al powders by HVOF spraying. As can be seen in Table 4, the photo-catalytic properties of the coatings from TiO_2 powder were excellent. On the other hand, the coatings from TiO_2-Al powder also had high photo-catalytic performance. Especially, the decomposition property of the coating fabricated under the fuel gas pressure of 0.20 MPa was equivalent to that of pure anatase powder.

4. Summary

TiO_2 photo-catalytic coatings were fabricated from TiO_2 and TiO_2-Al agglomerated powders by thermal spraying. The effects of addition of aluminum on the fabrication and characteristics of TiO_2 coatings were investigated. The results are summarized as follows.

(1) Due to the addition of aluminum, thick coatings were formed even at low heat input conditions both in plasma and HVOF spraying. In the plasma spraying process, however, Ti_3O_5 and magneli phase were formed in the coatings because of deoxidization of TiO_2 by aluminum. As a result, the photo-catalytic efficiency of coatings from TiO_2-Al powder were worse by two orders than those from pure anatase TiO_2 powder.

(2) The thick coatings with high anatase ratio could be fabricated from TiO_2-Al powder by HVOF spraying. The surfaces of these specimens were covered with powder-like TiO_2 particles and the coating thickness was 50 μm. The photo-catalytic properties of these coatings were equivalent to that of pure anatase powder.

References

[1] A. Fujishima and K. Honda, Nature, Vol. 238, (1972), p.37-38.

[2] I. Sopyan, M. Watanabe, S. Murasawa, K. Hashimoto and A. Fujishima, Journal of Photochemistry and Photobiology A:Chemistry, Vol. 98, (1996), p.79-86.

[3] A. Mills and J. Wang, Journal of Photochemistry and Photobiology A:Chemistry, Vol. 127, (1999), p.123-134.

[4] K. Tanaka, T. Hisanaga and A. P. Rivera, Photocatalytic Purification and Treatment of Water and Air, (1993), p.169-178.

[5] X. Liu, J Yang, L. Wang, X. Yang, L. Lu and X. Wang, Materials Science and Engineering A, Vol. 289, (2000), p.241-245.

[6] C. Garzella, E. Comini, E. Tempesti, C. Frigeri and G. Sberveglieri, Sensors and Actuators B:Chemical, Vol.68, (2000), p.189-196.

[7] TRC R&D Library, Latest Technological Trend of Photo-Catalyst, Shimeiko Publishing, Tokyo, (1998), (in Japanese).

[8] A. Ohmori, H. Shoyama, S. Matsusaka, K. Ohashi, K. Moriya and C. J. Li, Proceedings of the 1st International Thermal Spray Conference, (2000), p.317-323.